Analysis of nickel distribution by synchrotron radiation X-ray fluorescence in nickel-induced early- and late-phase allergic contact dermatitis in Hartley guinea pigs

Shan-Qun Jiang[1], Xiang-Yu Wu[1], Jin-Lyu Sun[2], Guang Chen[3], Rui Tang[2], Zhi Li[2], Ruo-Yao Wei[4], Lan Liang[2], Xian-Jie Zhou[2], Dong-Liang Chen[3], Jun Li[5], Hong Gao[4], Jing Zhang[3], Zuo-Tao Zhao[6]

[1]School of Life Science, Anhui University, 111 Jiulong Road, Hefei, Anhui 230601, China;
[2]Department of Allergy, Peking Union Medical College Hospital, Chinese Academy of Medical Sciences (CAMS) & Peking Union Medical College (PUMC), Beijing Key Laboratory of Precision Medicine for Diagnosis and Treatment on Allergic Diseases, Beijing 100730, China;
[3]Beijing Synchrotron Radiation Facility (BSRF), Institute of High Energy Physics, Chinese Academy of Sciences, Beijing 100049, China;
[4]The Institute of Laboratory Animal Science, Chinese Academy of Medical Sciences (CAMS) & Peking Union Medical College (PUMC), Beijing 100021, China;
[5]Laboratory Animal Center, Peking University, Beijing 100083, China;
[6]Department of Dermatology, Peking University First Hospital, Peking University, Beijing Key Laboratory of Molecular Diagnosis on Dermatoses, Beijing 100034, China.

Abstract

Background: Nickel-induced allergic contact dermatitis (Ni-ACD) is a global health problem. More detailed knowledge on the skin uptake of haptens is required. This study aimed to investigate the penetration process and distribution of nickel in skin tissues with late phase and early phase of Ni-ACD to understand the mechanisms of metal allergy.

Methods: Forty Hartley guinea pigs were divided into four groups according to the $NiSO_4$ sensitizing concentration and the $NiSO_4$ challenged concentration: the 5% $NiSO_4$-group, 5% to 10% (sensitization-challenge; late phase group); 10% $NiSO_4$-group, 10% to 10% (sensitization-challenge; early-phase group); and the positive and negative controls. Pathological biopsies were performed on each group. The depth profile of nickel element concentration in the skin of guinea pigs was detected by synchrotron radiation micro X-ray fluorescence spectroscopy (SR-μ-XRF) and micro X-ray absorption near-edge spectroscopy (μ-XANES).

Results: In each section, the nickel element concentration in both the 5% $NiSO_4$-group and 10% $NiSO_4$-group was significantly higher than that in the negative control group. In the upper 300-μm section of skin for the early phase group, the nickel element concentration was significantly higher than that in the lower section of skin. In deeper sections (>200 μm) of skin, the concentration of nickel in the early phase group was approximately equal to that in the late phase group. The curve of the late phase group was flat, which means that the nickel element concentration was distributed uniformly by SR-μ-XRF. According to the XANES data for the 10% $NiSO_4$ metal salt solution, structural changes occurred in the skin model sample, indicating that nickel was not present in the Ni^{2+} aqueous ionic state but in the nickel-binding protein.

Conclusions: This study showed that the distribution of the nickel element concentration in ACD skin tissue was different between the early phase and late phase groups. The nickel element was not present in the Ni^{2+} aqueous ionic state but bound with certain proteins to form a complex in the stratum corneum in ACD model tissue.

Keywords: Synchrotron radiation micro X-ray fluorescence spectroscopy; Micro X-ray absorption near-edge spectroscopy; Dermatitis, Allergic contact; Nickel-induced allergic contact dermatitis; Dermatology

Introduction

Contact allergies represent a common form of dermatitis worldwide, especially in developed countries such as the United States and Europe.[1] Nickel is a common contact allergen on patch testing in western countries, and it affects 10% of women and 1% to 2% of men.[2] The differences between sexes were mainly explained by an increased frequency of jewelry exposure in women. Despite efforts to minimize prevalence, for example, by nickel restriction within the Europe,[3] up to 21% of the market accessories studied were found to release nickel.[4] In coins made of alloys, nickel was detected, and the concentration of nickel was beyond the safe exposure threshold.[5] Thus, the stresses caused by exposure to nickel are still high.

Within the past few decades, the interest in nickel among scientists has increased as a result of the progressive

Access this article online

Quick Response Code:

Website: www.cmj.org

DOI: 10.1097/CM9.0000000000000365

Correspondence to: Dr. Jin-Lyu Sun, Department of Allergy, Peking Union Medical College Hospital, Chinese Academy of Medical Sciences (CAMS) & Peking Union Medical College (PUMC), Beijing Key Laboratory of Precision Medicine for Diagnosis and Treatment on Allergic Diseases, Beijing 100730, China
E-Mail: sunjinlv@pumch.cn

Chinese Medical Journal 2019;132(16)

Received: 05-03-2019 **Edited by:** Yuan-Yuan Ji

industrial and commercial significance of nickel as well as the improvement of analytical methods for nickel by electrothermal atomic absorption spectrometry. Currently, measurements in many countries, including China, indicate that the concentrations of nickel in the environment (air, water, soil, and food) do not exceed legislative limits and should not be dangerous for the general population.[6] However, people should keep in mind that, at present, nickel, although not released extensively into the environment, may represent a hazard to human health.

Nickel elements are potent allergens or haptens that can trigger skin inflammation, and nickel can penetrate through the stratum corneum to the epidermis. Therefore, efforts have been undertaken to investigate the penetration and distribution of haptens through the skin. Synchrotron radiation X-ray fluorescence spectroscopy (SR-XRF) and micro-focused particle-induced X-ray emission were used to analyze nickel allergy patch application in normal mouse skin.[7] Time of flight secondary ion mass spectrometry was used for investigation of the penetration and distribution of nickel in normal human skin.[8] Although these nickel-exposed animals developed metal allergy, the precise mechanism underlying this allergy remains unknown.

As reported, metal allergy is an inflammatory disease categorized as a delayed-type hypersensitivity reaction, in which skin inflammation is mediated by hapten-specific T cells.[9,10] Therefore, there is a need to identify the clinical relevance and the elemental- and chemical-specific distribution of nickel within tissues. This study investigates the internal distribution of nickel in skin tissues with nickel-induced allergic contact dermatitis (Ni-ACD) using microprobe-SR-XRF to identify the spatial distribution of nickel and its colocalization with endogenous elements. X-ray absorption near-edge structure (XANES) spectroscopy can also be used to determine the oxidation state of nickel bound to the biotic ligands. This study used correlative microprobe SR-XRF and XANES to investigate the penetration process and distribution of nickel in skin tissues with late phase and early phase of Ni-ACD to understand the mechanisms of metal allergy.

Methods

Ethical approval

Forty Hartley guinea pigs were used in the study after approval by the Animal Care and Use Committee of the Institute of Laboratory Animal Science of Peking Union Medical College (No. ILAS-GLP-2013-042). All procedures used in this study were in accordance with our institutional guidelines that complied with the international ethics and humane standards for animal use. Every effort was made to minimize the number of animals and reduce their suffering.

Animals

Half male and half female Hartley guinea pigs (wide type genetic), weighing 240 to 270 g, were purchased from Beijing Vital River Laboratory Animal Technology Co., Ltd.: a joint venture of Charles River Laboratories in China. The animals were housed in individual cages, maintained under standardized conditions. The animals were given free access to filtered tap water and food and were maintained in specific pathogen-free conditions in our animal facility with a 12-h light/dark cycle.

Chemicals

Nickel sulfate (5% and 10%) ($NiSO_4 \cdot 6H_2O$ analytical grade, Xilong Chemical Co. Ltd, Beijing, China) was prepared in synthetic perspiration (SP) formulations (0.01 g/mL sodium chloride, 0.005 g/mL ammonium chloride, 0.005 g/mL urea, 0.0025 g/mL acetic acid, and 0.005 g/mL lactic acid was adjusted to pH 5.5 by the addition of ammonia). 2,4-Dinitrochlorobenzene (DNCB) was prepared with 1% acetone (Beijing Chemical Works, Beijing, China). Normal saline (NS) (Beijing Chemical Works) was prepared before the study.

Treatments

The animals were randomly assigned to either the test or the control group by the random number table. The random allocation sequence was generated and was concealed from the main investigator. Guinea pigs were allowed to acclimate for 1 week before use. Aliquots of the nickel sulfate solution (0.1 mL) were administered percutaneously to a clipped and shaved skin area (3× 3 cm) located on the left flank of the animals. The animals were treated three times on days 0, 1, and 2 for the sensitizing phase; the treated areas were patched for 6 h. The animals were challenged by occlusive patch tests on the right flank site using the previously described nickel sulfate solution on the shaved skin area on day 7. The treated areas were under occlusion for 24 h. After the challenge, we waited for 24 h and then recorded delayed hypersensitive response. In this study, we observed the skin change of 24 h (defined as early phase) and 72 h (defined as late phase), then we collected these skin biopsies after patch removement.

Control guinea pigs were treated with 1% to 1% (sensitization-challenge) DNCB in acetone and NS as the positive and negative control (NC) groups, respectively, and were challenged under identical conditions on day 7.

Skin reaction (erythema and swelling) evaluation

The evaluation time should be the immediate time of the removement of the patch and at least 24 h later to observe the delayed hypersensitive response. Skin reaction (erythema and swelling) was recorded by visual assessment after challenge. The intensity of the reaction was scored according to the following criteria[11]: 0, no visible change; 1, slight or discrete erythema and barely visible swelling; 2, moderate and confluent erythema and visible border swelling; 3, intense erythema and swelling; and 4, purplish-red eschar and over 1 mm of swelling. Response score averages were calculated for each group. Swelling and erythema were also documented by photography.

Skin specimen preparation

The patch was removed, and the flank skin was gently wiped after the guinea pigs were sacrificed. The skin that contacted the patch test was excised and gently wiped in each group. The specimen was cut into sections (5× 5 mm, 1 mm thick) and fixed in 10% neutral buffered formalin for use. The sectioned specimens in the 5% $NiSO_4$-group, 10% $NiSO_4$-group and NC group were placed on Kapton film (12.5 μm; Du Pont-Toray, Tokyo, Japan) and subjected to elemental distribution analyses. After that, specimen slices in all groups were embedded in paraffin blocks and subjected to hematoxylin and eosin (H&E) (Beijing Chemical Works) staining for histopathological analysis. Stained tissues were observed using a light microscope (original magnification ×40).

SR-μ-XRF spectroscopy

The micro X-ray fluorescence (μ-XRF) spectroscopy experiment was performed at 4W1B beamline, at the Beijing Synchrotron Radiation Facility (BSRF), which runs 2.5 GeV electron with current from 150 to 250 mA. The incident X-ray energy was monochromatized by W/B4C double-multilayer-monochromator at 15 keV and was focused down to 50 μm in diameter by the polycarpellary lens. Two-dimensional mapping was acquired by step-mode: the sample was held on a precision motor-driven stage, scanning 100 μm stepwise. The Si (Li) solid-state detector was used to detect X-ray fluorescence emission lines with a live time of 100 s. Here, XRF scans of the first point (0 μm) were determined to be at the position of the maximum change point of the profile. Data reduction and processing were performed using the PyMca package, which is freely distributed for non-commercial applications, and the code can be downloaded from http://www.esrf.fr/computing/bliss/downloads.[12]

SR-μ-XANES spectroscopy

The XANES experiments at a 1W2B wiggler beamline of BSRF were performed, where the storage ring was run with electrons at an energy level of 2.5 GeV and 150 to 250 mA ring current. The micro-XANES spectra (irradiated spot 50× 50 μm) at the nickel K-edge of the skin sample were collected in fluorescence mode using a Vortex-EM silicon drift detector. The XANES spectrum of the reference nickel ion solution (10% $NiSO_4$) was also collected in fluorescence mode for comparison. The photon energy was calibrated against the K-edge of nickel foil at 8333 ± 0.3 eV. The spectra were processed using Bruce Ravel's program ATHENA based on Matt Newville's IFEFFIT library.

Statistical analysis

Statistics analysis was performed with SPSS 18.0.0 software (IBM Corporation, Armonk, New York, USA) and Prism 7.0 software (GraphPad, La Jolla, CA, USA). The animals were randomly assigned to either the test or the control group by the random number table. The random allocation sequence was generated and was concealed from the main investigator. Kolmogorov-Smirnov test was used to test the normality of samples. To analyze the evaluation of erythema, we used the non-parametric Mann-Whitney *U* test, data were presented as median (Q1, Q3). To compare the fluorescence intensity of nickel, the Student's *t* test was used for statistical analysis. Data were presented as mean ± standard deviation. Levene test was used to test equality of variances. If the variances were heterogeneity, we used the Welch approximate *t* test to analyze data. A $P < 0.05$ was considered statistically significant.

Results

Skin reactions (erythema and swelling)

Figure 1 shows the evaluation of erythema surrounding skin reactions in all study groups during the experimental time periods (at 6, 12, 24, 48, and 72 h after the challenge). The average erythema scores peaked at 24 h in 5% to 10% group (sensitization-challenge $NiSO_4$ solution) and 10% to 10% group (sensitization-challenge $NiSO_4$ solution). At 12 h, the score in the 10% to 10% group was significantly higher than that in the 5% to 10% group (3 [2, 3] *vs.* 1 [1, 1], $Z = -3.953$, $P < 0.0001$). The skin reaction in two groups simultaneously declined gradually after 24 h. These symptoms disappeared after 72 h in two groups.

Pathohistological images of skin tissues

The H&E stained histopathological images from the skin cross-sections treated with patches for 24 h are shown in Figure 2. Gross changes observed by the naked eye revealed that the allergic responses on the surface of the skin tissues of guinea pigs were erythema and scabbing, which are likely due to the itching and redness found in patients with nickel ACD, with different degrees of change observed. In the late phase group, we observed late-phase histological features such as epidermal thickening, hyperkeratosis, and/or para-asteatosis and acanthosis in the epidermis, as well as angiotelectasis and inflammatory cell infiltration in the epidermis and dermis. Histopathological findings included hyperkeratosis with parakeratosis,

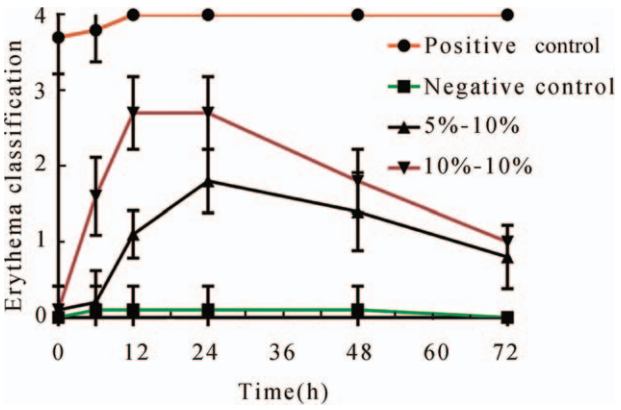

Figure 1: Evaluation of erythema in guinea pigs at different times after challenge. Skin reaction in animal model was correlated with clinical symptom scores with Magnusson and Kligman test's standard. Dot plots show values for average symptom scores in each group (ten Hartley guinea pigs) during 72 h. Data represent at least three independent experiments. The detected data was converted to average value in each group.

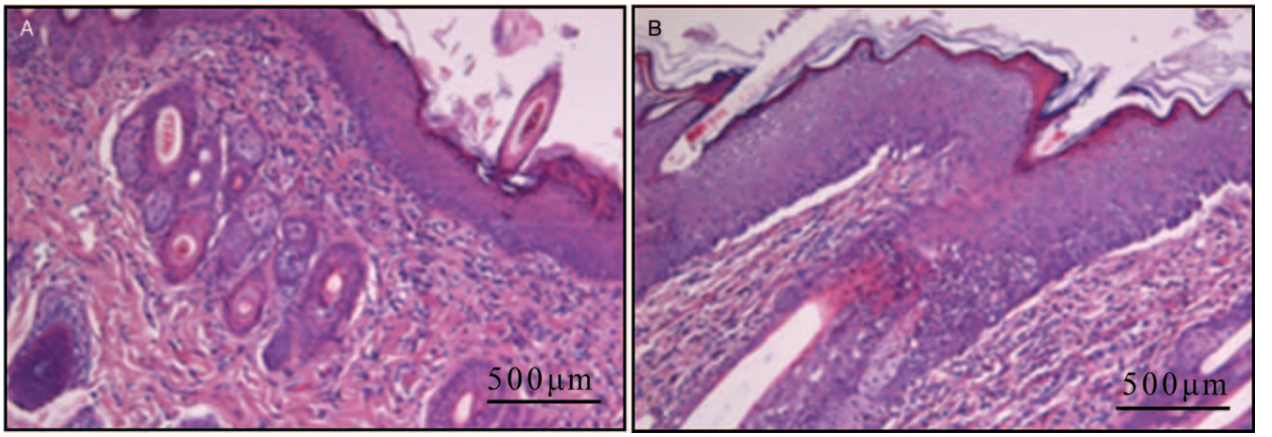

Figure 2: Pathological alterations in skin of model after challenge with $NiSO_4$ at 24 h. Hematoxylin and eosin staining of skin sections from early-phase group (A) and acute phase group (B) showed epidermis, dermis, and peri-vascular hypodermis infiltration of inflammatory symptoms in animal model at 24 h. Stained tissues were observed using a light microscope (original magnification ×40). Scale bars: 500 μm.

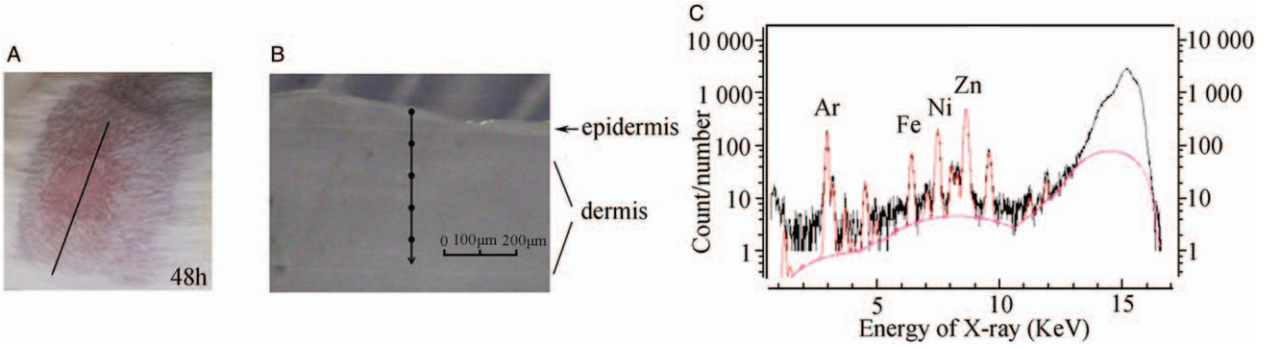

Figure 3: The main elements of skin tissues in guinea pigs-model after 48 h treatment. The images showed clear peaks for not only Ni, but also the metal elements Fe and Zn in the skin cross-sections after 48 h. Ar is non-metal element in air, it was not considered in this study. (A) The macroscopic image showed the skin section of animal. (B) Skin cross-section from animals (original magnification ×8, scale bars: 100 μm). The arrow points to direction of scanning before administering SR-XRF. (C) SR-XRF indicated the main elements from the skin cross-sections. The intensity of the element in negative control was regard as the background (pink line). SR-XRF: Synchrotron radiation X-ray fluorescence spectroscopy.

epidermal hyperplasia, dermal telangiectasia, and hyperemia [Figure 2]. In the early phase group, with 24 h challenge, there was substantially more inflammatory cell infiltration in the dermis than that in the late phase group. The skin lesions showed intra-cellular edema, liquefaction, and denaturation of the basal layer, as well as dermis vasodilatation and dermal cell infiltration.

Distribution of nickel element by SR-XRF from skin cross-sections

SR-XRF of the main elements from the skin cross-sections [Figure 3] showed clear peaks for not only nickel but also the metal elements Fe and Zn. The significantly higher signal intensity of nickel suggested the feasibility of the Ni-induced ACD model. The depth-resolved XRF was acquired to determine the distribution of nickel in the ACD model tissue. The photon energy corresponds to absorption above the Ni K edge excitation threshold and should be independent of any change in white line intensity due to oxidation state variation. The fluorescence intensity was proportional to the concentration of nickel [Figure 4]. In the early phase group, the content of nickel increased from 0 to 200 μm (epidermis in Figure 2), and it decreased gradually with deeper position. In contrast, the content of nickel element in the late phase group was slightly reduced and showed a stable fluctuation over the full depth. Obviously, within the deep position of 200 μm, the nickel content in the early phase group was much higher than that in the late phase group ($0.00092 \pm 1.961 \times 10^{-5}$ *vs.* $0.00053 \pm 9.487 \times 10^{-6}$, $t = 17.91$, degree of freedom [df] = 13.00, $P < 0.0001$). In deeper positions of 500 μm, the nickel element concentration in the two groups was approximately similar ($0.00040 \pm 9.803 \times 10^{-6}$ *vs.* $0.00038 \pm 1.992 \times 10^{-5}$, $t = 0.90$, df = 13.12, $P = 0.380$) [Figure 4]. These results suggested that the permeated nickel content was concentrated in the epidermis first. Then, the content penetrated to the dermis beyond the basal layer, especially in the early phase group.

Chemical species of nickel element in the skin model by SR-XANES

XANES studies were performed to investigate the nickel binding properties in ACD model tissues [Figure 5]. The comparison of the XANES data for nickel in the 10% $NiSO_4$ solution and the ACD model tissue showed that a structural change occurred in the nickel site. Nickel had

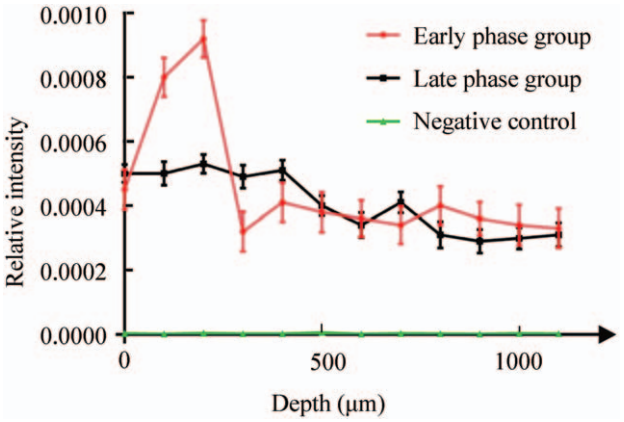

Figure 4: The relative comparison of nickel content in skin tissues of Ni-ACD model. The depth-resolved XRF were acquired to determine the distribution of Ni in the ACD model tissue. XRF scan of first point (0 μm) was determined to be at the position of maximum change point of the profile. Values represent at least three independent experiments and the detected data was converted to average value in each group. Ni-ACD: Nickel induced allergic contact dermatitis; XRF: X-ray fluorescence spectroscopy.

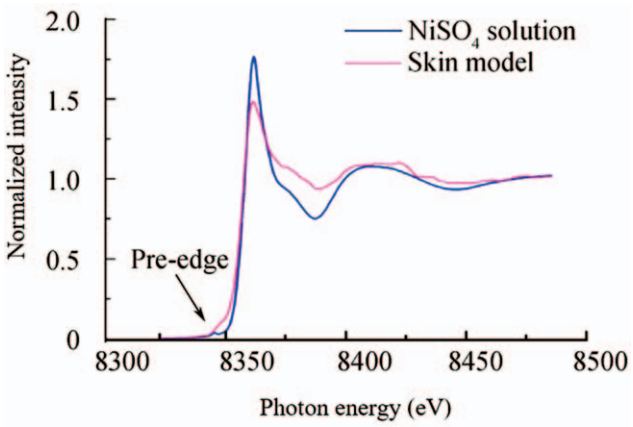

Figure 5: X-ray absorption near-edge spectroscopy of nickel K edge in the skin of Ni-ACD. XANES studies were performed to investigate the nickel binding properties in this model tissue. The peaks will depend on the coordination number and geometry of the metal site. The difference was observed between the ACD model tissue (Skin model) and the 10% $NiSO_4$ solution ($NiSO_4$ solution). Ni-ACD: Nickel induced allergic contact dermatitis; XANES: X-ray absorption near-edge spectroscopy.

vacancies in the 3*d* manifold, and peaks associated with 1*s*–3*d* transitions were observed in the pre-edge XANES for nickel in the 10% $NiSO_4$ solution [Figure 5], suggesting that nickel was in the aqueous ionic state. In the case of ACD model tissues, small shoulders associated with peaks involving 1*s*–4*pz* transitions were observed. The peaks depended on the coordination number and geometry of the metal site. By comparing the peaks with samples of known coordination numbers and geometries, nickel in ACD model tissue was not present in the Ni^{2+} aqueous ionic state but in nickel-binding protein.[13]

Discussion

In the present study, Ni-induced ACD models were produced by modified protocols with SP formulations for guinea pigs based on traditional skin sensitization methods. We used SR-XRF to investigate the distribution of the nickel element in the skin tissues of two different Ni-ACD models (late phase and early phase), and the chemical species of the nickel element was also revealed via SR-XANES. In addition, H&E stained imaging of the target tissue sections provided histopathological information. Hence, the feasibility of these models and the distribution of metal permeation behavior in the skin tissues was confirmed.

Ni-ACD is a type IV allergy reaction.[14] For a hapten to be able to initiate this reaction, it has to penetrate through the stratum corneum to the epidermis.[15] Therefore, efforts have been undertaken to investigate the penetration and distribution of haptens through the skin.[11,14,16-18] For normal human and mouse skin, imaging mass spectrometry and SR-XRF were used to analyze the penetration and distribution of nickel.[7,8] However, these methods do not give detailed information on nickel element penetration and distribution in the skin in the pathogenesis of contact dermatitis. Therefore, there is a need to investigate clinically relevant haptens and their distribution in the epidermis of contact dermatitis with non-destructive inspection.

The evaluation of erythema on skin reactions is used to judge the concentration of nickel indirectly.[19] According to our study, we found that symptoms were dependent on the time of nickel penetration. An *in vitro* study evaluating nickel element permeation through the human stratum corneum also reported that the permeation rate of aqueous $NiSO_4$ solution was the highest after approximately 24 h, regardless of the nickel salt species, which is in agreement with our results.[8]

The two groups, including both early phase and late phase ACD models, displayed different symptoms during the experiment. For each depth of skin, the nickel element concentration in the early phase group was higher than that in the late phase group. In our study, it was observed that the skin nickel element concentration from 100 to 200 μm depth in the early phase group was higher than that under 300 μm depth. Similar results were also found by Sugiyama *et al*.[7] However, the lord-balanced permeated nickel was diffused in the cross-section of the late phase group. The concentration of nickel caused this phenomenon. Permeation of high concentrations of nickel into the skin was reported to increase blood flow.[20,21] Thus, the removal of nickel-binding proteins by blood flow may keep nickel concentration well-balanced under deeper tissues. Corresponding to the evaluation of erythema in skin reactions, the states of swelling and skin lesions contributed to the depth of tissues, which might enlarge scales of the stratum corneum and epidermis in a severe lesion condition.

Comparing the XANES data for the 10% $NiSO_4$ solution treatment, structural changes occurred in the skin model sample. We demonstrated that nickel was not present in the Ni^{2+} aqueous ionic state but bound to nickel-binding proteins *in vivo*. Some reports found and proved this phenomenon of nickel metal-binding amino acids, peptides, or proteins *in vitro*.[22-24] Our study demonstrated nickel binding events for nickel contact allergy *in vivo* by the measurement of XANES. Some relative studies have reported that Ni^{2+} triggered an inflammatory response by

directly activating human Toll-like receptor 4 (TLR4) *in vitro*, and they demonstrated that Ni^{2+}-induced ACD symptoms were species-specific, as the mouse TLR family could not generate this response; mouse TLR senses microbial pathogens and endogenous ligands.[13,25] A recent study has reported that nickel (II) ions bind particularly at histidine residues, which are in the region required for the recognition of nickel signals.[26] However, it is not clear which proteins of hapten Ni^{2+} were combined to trigger Ni-induced ACD. Future research is required to explore this further.

In conclusion, this study showed that the distribution of the nickel element in ACD skin tissue was different between the early phase and late phase groups. The nickel element was not present in the Ni^{2+} aqueous ionic state but bound with certain proteins to form a complex in the stratum corneum nickel in ACD model tissue. SR-XRF and XANES technologies were non-invasive, and depth-resolved structure analysis was used for the conventional histopathological specimens. Therefore, these technologies may be applicable for the screening of metal-affected lesions and the evaluation of the effects of permeated metal elements on skin tissue lesions.

Acknowledgements

The authors thank Bo Chen at pathology department of Peking Union Medical College Hospital, Chinese Academy of Medical Sciences (CAMS) for giving advices in this study.

Funding

This research was supported by the grants from National Natural Science Foundation of China (No. 81373175), and CAMS Innovation Fund for Medical Sciences (No. 2016-I2M-1003).

Conflicts of interest

None.

References

1. Thyssen JP, Linneberg A, Menné T, Johansen JD. The epidemiology of contact allergy in the general population–prevalence and main findings. Contact Dermatitis 2007;57:287–299. doi: 10.1111/j.1600-0536.2007.01220.x.
2. Thyssen JP, Linneberg A, Menné T, Johansen JD. Quantitative aspects of nickel dermatitis. Sensitization and eliciting threshold concentrations. Sci Total Environ 1994;148:275–281. doi: 10.1016/0048-9697(94)90403-0.
3. Spiewak R, Pietowska J, Curzytek K. Nickel: a unique allergen–from molecular structure to European legislation. Expert Rev Clin Immunol 2007;3:851–859. doi: 10.1586/1744666X.3.6.851.
4. Ahlström MG, Menné T, Thyssen JP, Johansen JD. Nickel allergy in a Danish population 25 years after the first nickel regulation. Contact Dermatitis 2017;76:325–332. doi: 10.1111/cod.12782.
5. Staton I, Ma R, Evans N, Hutchinson RW, McLeod CW, Gawkrodger DJ. Dermal nickel exposure associated with coin handling and in various occupational settings: assessment using a newly developed finger immersion method. Br J Dermatol 2006;154:658–664. doi: 10.1111/j.1365-2133.2006.07128.x.
6. Denkhaus E, Salnikow K. Nickel essentiality, toxicity, and carcinogenicity. Crit Rev Oncol Hematol 2002;42:35–56. doi: 10.1016/s1040-8428(01)00214-1.
7. Sugiyama T, Uo M, Wada T, Hongo T, Omagari D, Komiyama K, *et al*. A method to visualize transdermal nickel permeation in mouse skin using a nickel allergy patch. Biomed Mater Eng 2015;26:1–8. doi: 10.3233/BME-151543.
8. Malmberg P, Guttenberg T, Ericson MB, Hagvall L. Imaging mass spectrometry for novel insights into contact allergy–a proof-of-concept study on nickel. Contact Dermatitis 2018;78:109–116. doi: 10.1111/cod.12911.
9. Mishra KP. Lead exposure and its impact on immune system: a review. Toxicol In Vitro 2009;23:969–972. doi: 10.1016/j.tiv.2009.06.014.
10. Thomas P, Braathen LR, Dörig M, Auböck J, Nestle F, Werfel T, *et al*. Increased metal allergy in patients with failed metal-on-metal hip arthroplasty and peri-implant T-lymphocytic inflammation. Allergy 2009;64:1157–1165. doi: 10.1111/j.1398-9995.2009.01966.x.
11. Schlede E, Eppler R. Testing for skin sensitization according to the notification procedure for new chemicals: the Magnusson and Kligman test. Contact Dermatitis 1995;32:1–4. doi: 10.1111/j.1600-0536.1995.tb00830.x.
12. Solé VA, Papillon E, Cotte M, Walter PH, Susini J. A multiplatform code for the analysis of energy-dispersive X-ray fluorescence spectra. Spectrochim Acta Part B At Spectrosc 2007;62:63–68. doi: 10.1016/j.sab.2006.12.002.
13. Chen H, Giri NC, Zhang R, Yamane K, Zhang Y, Maroney M, *et al*. Nickel ions inhibit histone demethylase JMJD1A and DNA repair enzyme ABH2 by replacing the ferrous iron in the catalytic centers. J Biol Chem 2010;285:7374–7383. doi: 10.1074/jbc.M109.058503.
14. Saito M, Arakaki R, Yamada A, Tsunematsu T, Kudo Y, Ishimaru N. Molecular mechanisms of nickel allergy. Int J Mol Sci 2016;17:202. doi: 10.3390/ijms17020202.
15. Karlberg AT, Bergström MA, Börje A, Luthman K, Nilsson JL. Allergic contact dermatitis–formation, structural requirements, and reactivity of skin sensitizers. Chem Res Toxicol 2008;21:53–69. doi: 10.1021/tx7002239.
16. Antonov D, Schliemann S, Elsner P. Agner T. Methods for the assessment of barrier function. Curr Probl Dermatol: skin barrier function Basel: Karger Publishers; 2016;61–70.
17. Chavalitnitikul C, Levin L. A laboratory evaluation of wipe testing based on lead oxide surface contamination. Am Ind Hyg Assoc J 1984;45:311–317. doi: 10.1080/15298668491399848.
18. Barratt MD, Basketter DA. Possible origin of the skin sensitization potential of isoeugenol and related compounds. (I). Preliminary studies of potential reaction mechanisms. Contact Dermatitis 1992;27:98–104. doi: 10.1111/j.1600-0536.1992.tb05217.x.
19. Antico A, Soana R. Chronic allergic-like dermatopathies in nickel-sensitive patients. Results of dietary restrictions and challenge with nickel salts. Allergy Asthma Proc 1999;20:235–242. doi: 10.2500/108854199778338991.
20. Wahlberg JE. Nickel: the search for alternative, optimal and non-irritant patch test preparations: assessment based on laser Doppler flowmetry. Skin Res Technol 1996;2:136–141. doi: 10.1111/j.1600-0846.1996.tb00075.x.
21. Wahlberg JE. Nickel chloride or nickel sulfate? Irritation from patch-test preparations as assessed by laser Doppler flowmetry. Dermatol Clin 1990;8:41–44. doi: 10.1016/s0733-8635(18)30519-9.
22. Medici S, Peana M, Nurchi VM, Zoroddu MA. The involvement of amino acid side chains in shielding the nickel coordination site: an NMR study. Molecules 2013;18:12396–12414. doi: 10.3390/molecules181012396.
23. Peana M, Medici S, Nurchi VM, Crisponi G, Zoroddu MA. Nickel binding sites in histone proteins: spectroscopic and structural characterization. Coord Chem Rev 2013;257:2737–2751. doi: 10.1016/j.ccr.2013.02.022.
24. Zoroddu MA, Peana M, Medici S, Anedda R. An NMR study on nickel binding sites in Cap43 protein fragments. Dalton Trans 2009;5:5523–5534. doi: 10.1039/b903305j.
25. Schmidt M, Raghavan B, Müller V, Vogl T, Fejer G, Tchaptchet S, *et al*. Nat Immunol 2010;11:814–819. doi: 10.1038/ni.1919.
26. Zoroddu MA, Peana M, Medici S, Potocki S, Kozlowski H. Ni (II) binding to the 429-460 peptide fragment from human Toll like receptor (hTLR4): a crucial role for nickel-induced contact allergy? Dalton Trans 2014;43:2764–2771. doi: 10.1039/c3dt52187g.

How to cite this article: Jiang SQ, Wu XY, Sun JL, Chen G, Tang R, Li Z, Wei RY, Liang L, Zhou XJ, Chen DL, Li J, Gao H, Zhang J, Zhao ZT. Analysis of nickel distribution by synchrotron radiation X-ray fluorescence in nickel-induced early- and late-phase allergic contact dermatitis in Hartley guinea pigs. Chin Med J 2019;132:1959–1964. doi: 10:4103/0366-6999.233964